Variational Quantum-Neural Hybrid Eigensolver

Shi-Xin Zhang,[1,2,*] Zhou-Quan Wan,[1,2,*] Chee-Kong Lee,[3] Chang-Yu Hsieh,[2,†] Shengyu Zhang,[2] and Hong Yao[1,‡]
[1]*Institute for Advanced Study, Tsinghua University, Beijing 100084, China*
[2]*Tencent Quantum Laboratory, Tencent, Shenzhen, Guangdong 518057, China*
[3]*Tencent America, Palo Alto, California 94306, USA*

(Received 6 June 2021; revised 22 August 2021; accepted 22 February 2022; published 24 March 2022)

The variational quantum eigensolver (VQE) is one of the most representative quantum algorithms in the noisy intermediate-scale quantum (NISQ) era, and is generally speculated to deliver one of the first quantum advantages for the ground-state simulations of some nontrivial Hamiltonians. However, short quantum coherence time and limited availability of quantum hardware resources in the NISQ hardware strongly restrain the capacity and expressiveness of VQEs. In this Letter, we introduce the variational quantum-neural hybrid eigensolver (VQNHE) in which the shallow-circuit quantum *Ansatz* can be further enhanced by classical post-processing with neural networks. We show that the VQNHE consistently and significantly outperforms the VQE in simulating ground-state energies of quantum spins and molecules given the same amount of quantum resources. More importantly, we demonstrate that, for arbitrary postprocessing neural functions, the VQNHE only incurs a polynomial overhead of processing time and represents the first scalable method to exponentially accelerate the VQE with nonunitary postprocessing that can be efficiently implemented in the NISQ era.

DOI: 10.1103/PhysRevLett.128.120502

Introduction.—Quantum computation was first envisioned by Feynman as a natural approach to efficiently simulate quantum systems [1]. Equipped with error resilient logical qubits in the fault-tolerant quantum computation regime [2], we can efficiently and arbitrarily precisely prepare the ground state of any given Hamiltonian by combining adiabatic evolution with quantum phase estimation [3,4]. However, this fault-tolerant strategy requires coherently operating an excessively large number of high-quality physical qubits with high precision that is beyond the realm of current technology [5]. Instead, in the noisy intermediate-scale quantum (NISQ) era [6], practical quantum computation is enabled by the hybrid quantum-classical scheme that dramatically alleviates the quantum hardware resources requirement to accomplish nontrivial computational tasks [7–9]. In such a scheme, the ground-state problem for a Hamiltonian, $\hat{H}$, is solved by preparing a quantum state in a parametrized quantum circuit (PQC) $U(\boldsymbol{\theta})$ as $|\psi_\theta\rangle = U(\boldsymbol{\theta})|0\rangle$. The parameters $\boldsymbol{\theta}$ are optimized to minimize $\langle\psi_\theta|\hat{H}|\psi_\theta\rangle$ and can be trained by a classical optimizer. This hybrid variational approach, usually called the variational quantum eigensolver (VQE), has been successfully applied to a wide range of molecular and quantum spin systems [10–17], as well as tasks of excited state search [18,19] and dynamical simulations [20–27]. Indeed, the VQE is regarded as one of the most promising routes toward practical quantum advantage [28,29] in the NISQ era.

To fully exploit the potential quantum advantage with the VQE, we should design a circuit *Ansatz* having a strong capacity for capturing quantum entanglements and correlations possibly present in the target quantum state. Two main categories of circuit *Ansatz* have been proposed for the VQE: physics inspired *Ansatz* and hardware efficient *Ansatz*. For physics inspired *Ansatz*, well-established quantum chemistry methods are adapted to the quantum computing context. For example, probably the most famous VQE *Ansatz*, unitary coupled cluster (UCC) *Ansatz* [10,11,30,31] is inspired by the coupled cluster method, a post-Hartree-Fock approach. Though the optimized state from UCC *Ansatz* can, in principle, give high accuracy when compared to the exact ground state, it requires a very deep circuit to implement for the following two reasons: (i) one needs to Trotterize the exponential operator, and (ii) the limited qubit connectivity in many chips, especially the ones with superconducting qubits, introduces a substantial depth overhead. Note that the circuit depth is a crucial measure in the NISQ era in order to accommodate the relatively short coherence time of qubits. To partially address the second issue, a hardware efficient *Ansatz* has been proposed [32]. The philosophy is to generate a quantum state by building a PQC with layers of native quantum gates available on a NISQ device that conforms to the connectivity of the hardware. While being easily implementable on current quantum hardware, the hardware efficient *Ansatz* has been reported to give inferior performance and accuracy [33]. Therefore, in the NISQ era, it is highly desired to devise novel approaches to substantially enhance the performance of the VQE while keeping the consumption of quantum resources such as circuit depth and number of quantum gates as low as possible.

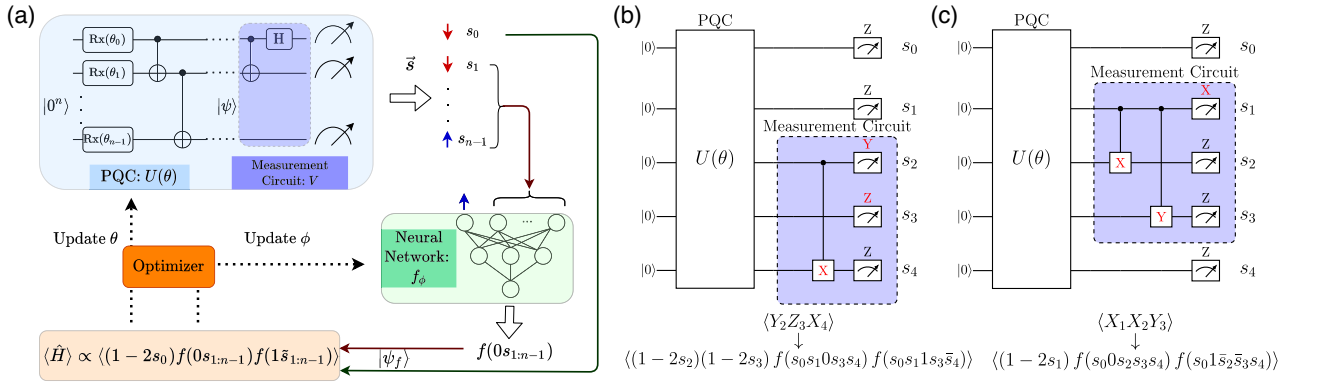

FIG. 1. (a) Schematic work flow for the VQNHE. The output state $|\psi\rangle = U(\boldsymbol{\theta})|0\rangle$ is attached with a small measurement circuit V. Measurement on computational (Z) basis is conducted on $VU(\boldsymbol{\theta})|0\rangle$ to collect shots of bit string result as $\vec{s}$. With the zeroth qubit as the star qubit (see main text for details), $0s_{1:n-1}$ and $1\tilde{s}_{1:n-1}$ are fed into the classical neural network f with trainable weights $\boldsymbol{\phi}$. The expectation of $\hat{H}$ can then be estimated according to Eq. (9). Finally, parameters in both PQC and the neural network are optimized with gradient based optimizer from the expectation result $\langle \hat{H} \rangle$. (b) Measurement protocol for $\hat{H} = Y_2 Z_3 X_4$. The star qubit corresponds to s_2 and the CX gate is applied to qubit 4 since X_4 is in $\hat{H}$. Meanwhile, CZ gate is omitted in the hardware level, and its effect is counted by the prefactor s_3 in the expression. (c) Measurement protocol for $\hat{H} = X_1 X_2 Y_3$. The star qubit corresponds to s_1. CX and CY gates are applied on qubits 2 and 3, respectively, since there are X_2 and Y_3 in $\hat{H}$.

One promising approach is to combine modern neural networks with quantum circuits in the hybrid quantum-classical paradigm. A few works have attempted to jointly train a classical neural network with a quantum computing module in order to boost the performance of various tasks [34–41]. In particular, the potential gain of introducing classical post-processing to a hybrid algorithm has been actively discussed in the field of quantum machine learning [42,43]. Different from classification and regression, the task for the VQE is to generate a quantum state rather than inferring a label or scalar. Since the quantum nature of the desired output is much harder to be embedded into a classical postprocessing framework, very few works have explored this possibility. In Ref. [44], the authors applied the so-called Jastrow factor [45] $\hat{\mathcal{P}}(\boldsymbol{\phi}) = \exp(\sum_{kl} \phi_{kl} Z_k Z_l)$ to the output state $|\psi_\theta\rangle$ of a quantum circuit, yielding the final target state $|\psi_f\rangle = \hat{\mathcal{P}}(\boldsymbol{\phi})|\psi_\theta\rangle$. However, existing proposals to supplement the standard VQE with $\hat{\mathcal{P}}(\boldsymbol{\phi})$ suffer from two main drawbacks. First, though the Jastrow factor is known for capturing quantum correlations in variational Monte Carlo (VMC) [46,47], it is not the most general form of postprocessing, and thus, the expressive power of such a setup is quite limited. More importantly, $\hat{\mathcal{P}}(\boldsymbol{\phi})$ cannot be straightforwardly implemented on a quantum computer. Existing methods proposed to evaluate $\langle \psi_f | \hat{H} | \psi_f \rangle$ require an exponential amount of times or resources to achieve the same measurement accuracy as the standard VQE [44]. Specifically, in the transformed Hamiltonian approach [48], the extra Jastrow operator is absorbed into the original Hamiltonian $\hat{H}$, and one needs to evaluate $\langle \psi | (\hat{\mathcal{P}}\, \hat{H}\, \hat{\mathcal{P}}) | \psi \rangle$. Since there is an exponential number of Pauli strings in the Taylor expansion of $\hat{\mathcal{P}}$, one has to evaluate exponential numbers of Pauli strings for the transformed Hamiltonian. (See the Supplemental Material [49] for a detailed analysis on the resources for these two approaches).

In this Letter, we introduce the variational quantum-neural hybrid eigensolver (VQNHE) which falls into the paradigm of variational quantum algorithms enhanced by classical postprocessing. Our approach successfully addresses both challenges encountered in the earlier attempts to combine the VQE with classical postprocessing: (i) the VQNHE possesses much greater expressive power as the post-processing can be modeled by any modern neural networks; (ii) the VQNHE utilizes the same amount of quantum resource as the original VQE while the classical overhead is provably polynomial in the output range of the neural function and constant in terms of problem size. We emphasize that the rigorously proven polynomial efficiency of the VQNHE is highly nontrivial as the nonunitary postprocessing overhead in this scenario is often thought to be intrinsically exponential. Therefore, our approach presents the first scalable method to exponentially accelerate the VQE with nonunitary postprocessing.

Setup and method.—The schematic work flow of the VQNHE is shown in Fig. 1(a). Suppose the output state from the PQC $U(\boldsymbol{\theta})$ is $|\psi\rangle = U(\boldsymbol{\theta})|0\rangle$. We propose the following nonunitary postprocessing operator:

$$\hat{f} = \sum_{s \in \{0,1\}^n} f_\phi(s) |s\rangle\langle s|, \tag{1}$$

where $f_\phi(s)$ is a parametrized function of a bitstring s. Then the (unnormalized) target output state from the

VQNHE is $|\psi_f\rangle = \hat{f}|\psi\rangle$. The aim is to minimize the energy expectation

$$\langle \hat{H} \rangle_f = \frac{\langle \psi_f | \hat{H} | \psi_f \rangle}{\langle \psi_f | \psi_f \rangle}, \tag{2}$$

by tuning variational parameters $\boldsymbol{\theta}$ in the PQC U and $\boldsymbol{\phi}$ in the neural network f. When $\hat{f}$ is applied to $|\psi\rangle$, it adjusts ψ_s, the quantum amplitude of $|\psi\rangle$ in the computational basis s. For example, the Jastrow factor can be regarded as a special case of Eq. (1) as $f(s) = \exp[-\sum_{ij} \phi_{ij}(1-2s_i)(1-2s_j)]$.

The key to enabling the above work flow is to efficiently evaluate Eq. (2). Since $\hat{H}$ can be decomposed to a summation of Pauli strings, it suffices to compute the expectation for each Pauli string and then add them up. For this reason, we will assume, without loss of generality, that $\hat{H}$ is a Pauli string in the following discussions.

First, the denominator of Eq. (2) is easy to estimate from measurements as

$$\langle \psi_f | \psi_f \rangle = \sum_{s \in \{0,1\}^n} |\psi_s|^2 |f(s)|^2. \tag{3}$$

The measurement protocol for Eq. (3) is straightforward: we simply measure the PQC U in the computational (Z) basis for multiple shots for s, and compute the expectation of $|f(s)|^2$. If the Pauli string $\hat{H}$ only contains I and Z operators, since $\langle s|\hat{H}|s'\rangle = H_s \delta_{ss'}$, the estimation for the numerator is also easy

$$\langle \psi_f | \hat{H} | \psi_f \rangle = \sum_{s \in \{0,1\}^n} |\psi_s|^2 |f(s)|^2 H_s. \tag{4}$$

The key advantage of the VQNHE is its efficient scheme for evaluating $\langle \psi_f|\hat{H}|\psi_f\rangle$ when $\hat{H}$ contains X or Y operators. In this case, we label one of the qubits in the Pauli string with X or Y operators as the star qubit, and we rearrange the star qubit as the zeroth qubit in the derivation below. We further label $|\tilde{s}\rangle$ as the bitstring that satisfies $\hat{H}|s\rangle = S(\tilde{s})|\tilde{s}\rangle$, where $S = \pm 1, \pm i$ is the sign factor for such a basis transformation under $\hat{H}$. For example, for $\hat{H} = X_0 Y_1 Z_2$, $\widetilde{|011\rangle} = |101\rangle$, and $S(101) = -i$. Since $\hat{H}^2 = 1$, all eigenvalues are ± 1 and $S(s)S(\tilde{s}) = 1$. Thus, the matrix form of $\hat{H}$ can be expressed as

$$\hat{H} = \sum_{\substack{s_0 = 0, \\ s_{1:n-1} \in \{0,1\}^{n-1}}} S(s)|s\rangle\langle\tilde{s}| + S(\tilde{s})|\tilde{s}\rangle\langle s|. \tag{5}$$

Note that the sum is over all bitstrings but with the star qubit fixed as $s_0 = 0$, and we use the shorthand notation $s \in 0 s_{1:n-1}$ for simplicity. The 2^n eigenvectors of $\hat{H}$ with eigenvalue ± 1 have simple forms $|\pm, s_{1:n-1}\rangle$

$$|+, s_{1:n-1}\rangle = \frac{1}{\sqrt{2}}[S(0 s_{1:n-1})|0 s_{1:n-1}\rangle + |1\tilde{s}_{1:n-1}\rangle], \tag{6}$$

$$|-, s_{1:n-1}\rangle = \frac{1}{\sqrt{2}}[S(0 s_{1:n-1})|0 s_{1:n-1}\rangle - |1\tilde{s}_{1:n-1}\rangle]. \tag{7}$$

We restrict f to real-valued functions for now, and for the general case of complex-valued postprocessing f, efficient estimation is also possible (see the Supplemental Material [49] for details). We have

$$\begin{aligned}
&\langle \psi_f | \hat{H} | \psi_f \rangle \\
&= \langle \psi | \left(\sum_{s \in 0 s_{1:n-1}} f(s) f(\tilde{s}) S(s) |s\rangle\langle\tilde{s}| + f(s) f(\tilde{s}) S(\tilde{s}) |\tilde{s}\rangle\langle s| \right) |\psi\rangle \\
&= \langle \psi | \left(\sum_{s \in 0 s_{1:n-1}} f(s) f(\tilde{s}) (|+,s\rangle\langle +,s| - |-,s\rangle\langle -,s|) \right) |\psi\rangle \\
&= \sum_{s \in 0 s_{1:n-1}} |\psi_{+,s}|^2 f(s) f(\tilde{s}) + |\psi_{-,s}|^2 [-f(s) f(\tilde{s})],
\end{aligned} \tag{8}$$

where $\psi_{\pm,s} = \langle \pm, s_{1:n-1}|\psi\rangle$.

To realize a measurement in the eigenbasis of $\hat{H}$, we attach a measurement circuit V after the original PQC $U(\boldsymbol{\theta})$ such that the computational basis measurement on the output from $VU(\boldsymbol{\theta})|0\rangle$ corresponds to the amplitude for $|\pm, s_{1:n-1}\rangle$, where the readout for the first (star) qubit represents the eigenvalue of $\hat{H}$ and the readout for the remaining $n-1$ qubits stands for $s_{1:n-1}$. Specifically, we require $V^\dagger|s\rangle \propto |\pm, s_{1:n-1}\rangle$ so that $\psi_{\pm,s} = \langle \pm, s_{1:n-1}|\psi\rangle = \langle s|VU(\boldsymbol{\theta})|0\rangle$. The problem is now reduced to efficiently building a measurement circuit V which gives $V^\dagger|s\rangle \propto [|0 s_{1:n-1}\rangle + (1-2s_0)\hat{H}|0 s_{1:n-1}\rangle]$. The building rules for this V circuit are (1) For all qubits present in the Pauli string $\hat{H}$ except the star qubit, we apply a control-$X/Y/Z$ gate with the control being the star qubit, and the choice of the control gate is determined by the Pauli operator acting on the corresponding qubit in $\hat{H}$. (Note that control-Z gate can be omitted and replaced by counting the extra sign $1-2s_i$ in the final expression.) (2) The star qubit is measured in the X or Y basis determined by the corresponding operator in $\hat{H}$, or equivalently speaking, the star qubit is attached with a single-qubit gate: Hadamard gate in the X case, and $\mathrm{Rx} = \exp(-\pi/4\, iX)$ rotation gate in the Y case, and then measured on the computational (Z) basis. We explicitly constructed the measurement circuit V for a few representative Pauli strings $\hat{H}$, as shown in Figs. 1(b) and 1(c). By appending the aforementioned compact measurement circuit V to $U(\theta)$ and collecting measurement results as bitstring s, the expectation value from the quantum-neural hybrid state is given by

$$\langle \hat{H} \rangle_{\psi_f} = \frac{\langle (1-2s_0) f(0 s_{1:n-1}) f(1 \tilde{s_{1:n-1}}) \rangle_{UV}}{\langle f(s)^2 \rangle_U}, \tag{9}$$

where bitstring s in the denominator is drawn from the PQC U, and bitsring s in the numerator is drawn from the PQC with the measurement circuit V appended.

The extra quantum resources compared to the original PQC for the VQE is at most $m-1$ two-qubit gates, where m is the number of X and Y operators in the Pauli string $\hat{H}$, and $m = O(1)$ for typical short-range interaction Hamiltonians. Besides, the number of measurement shots required to achieve the same accuracy as the VQE is polynomially bounded (see the Supplemental Material [49] for details of a rigorous proof). Now that we can efficiently evaluate $\langle \hat{H} \rangle_{\psi_f}$, the gradients with respect to the PQC and the neural network can be efficiently obtained via parameter shift [50–52] and back propagation, respectively, which facilitate gradient-based classical optimizers to update parameters $\boldsymbol{\theta}$ and $\boldsymbol{\phi}$.

With the presented formalism and protocol, we have demonstrated that the VQNHE, the combination of the variational quantum eigensolver and classical nonunitary neural postprocessing, gives rise to an exponential acceleration compared to previous methods that incorporate nonunitary postprocessing into the VQE.

Results.—In this section, we report the performance of the VQNHE on several benchmarks in modeling quantum spins and molecules, including the 1D transverse field Ising model (TFIM), 1D Heisenberg model, LiH, H_6-hexagon and H_6-chain molecule [53]. (See the Supplemental Material [49] for details on the setup and results for each system.)

First, we present numerical results for quantum spin models: the TFIM defined as $H_{\mathrm{TFIM}} = \sum_{i,i+1} Z_i Z_{i+1} - \sum_i X_i$, and the Heisenberg model defined as $H_{\mathrm{Heisenberg}} = \sum_{i,i+1}(X_i X_{i+1} + Y_i Y_{i+1} + Z_i Z_{i+1})$, both imposed with the periodic boundary condition. We apply both the VQNHE and VQE to simulate the ground state of these systems with $N = 12$ sites. The results for the ground-state energy of these two systems are summarized in Table. I. Note that the VQNHE provides a substantially more accurate estimation (about 2 orders of magnitude improvement in terms of energy estimation accuracy) of the ground-state energy using the same amount of quantum resources.

TABLE I. The ground state energies obtained from both the VQE and VQNHE with the same PQC structure for 1D TFIM and the Heisenberg model with $N = 12$ sites. Relative errors compared to the exact ground state are included. For both models, the energy obtained from the VQNHE is much closer to the exact ground state energy than the one obtained from the VQE.

Model	TFIM	Heisenberg model
VQE	-14.914 (3×10^{-2})	-21.393 (7×10^{-3})
VQNHE	-15.319 (2×10^{-4})	-21.546 (2×10^{-4})
Exact	-15.3226	-21.5496

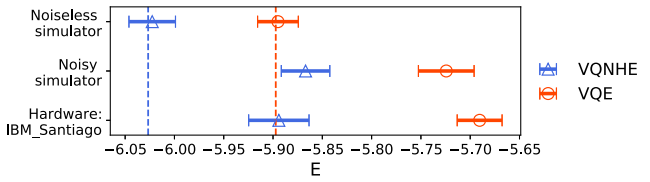

FIG. 2. Optimized energies on the five-site TFIM model with open boundary condition using either VQNHE (blue) and VQE (red) approaches. Measurement-based results in noiseless, noisy simulators, and real quantum hardware are shown with the error bar. The vertical red and blue lines are the ideal optimized energy values from the VQNHE and VQE, when no quantum noise or measurement uncertainty exists. The blue line also coincides with the exact ground state energy since the ideal VQNHE result has a relative error in the order of 10^{-12}.

We further obtain the optimized energies from the VQE and VQNHE algorithms simulated on IBM quantum hardware and noisy simulators, as shown in Fig. 2. The target model is the five-site TFIM model with an open boundary condition. The results demonstrate that the VQNHE works well in the presence of quantum noise and measurement uncertainty on the real quantum hardware.

Now, we turn to the calculation of the energy dissociation curve for LiH, another common benchmark for the

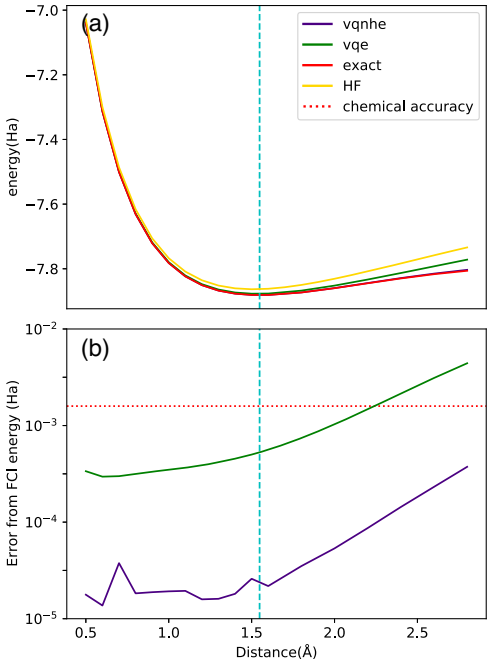

FIG. 3. LiH dissociation curve. (a) VQNHE optimized energy (purple), VQE converged energy (green), exact energy from full configuration interaction (red), Hartree-Fock (HF) energy (yellow) obtained at different bond distances. (b) Comparison of corresponding energy errors for VQNHE and VQE results. The red dash line is the threshold of chemical accuracy. The cyan vertical line is the bond distance with minimum bonding energy, representing LiH molecule at equilibrium configuration.

VQE. We optimize LiH qubit Hamiltonian using the VQNHE and VQE with 20 independent runs for each bond distance from 0.5 to 2.8 Å, and the best results of each instance are reported in Fig. 3. Both the VQNHE and VQE utilize the same hardware efficient *Ansatz*. The relative error of the VQNHE result is in the order of 10^{-5}, matching the state-of-the-art result by restricted Boltzmann machine-based VMC [56]. For comparison, the vanilla VQE can only achieve a relative error around the order of 10^{-3}.

Furthermore, we apply the VQNHE on the molecular system H_6-hexagon and H_6-chain. Via symmetry enforced qubit encoding [57], we can simulate the corresponding system with a ten-qubit PQC and complex-RBM based postprocessing module. The relative errors of optimized energy for both systems are in the order of 10^{-5} and 10^{-6}, respectively. Our VQNHE results are not only within chemical accuracy, but actually outperform the coupled cluster singles and doubles method.

Discussions.—The VQNHE presented in this Letter sits at the intersection between the VQE and VMC [58–60]. It is similar to the VMC setup for a complex-valued wave function, where two computational graphs are utilized: one is for the amplitude and the other one is for the phase or sign structure. Since the quantum phase is harder to characterize than the amplitude [61–63], tensor network *Ansätze* have been proposed to capture such subtlety as a replacement of the neural network [64]. Within the VQNHE framework, we can view the PQC $U(\boldsymbol{\theta})$ as the part responsible for learning quantum phase. Since the PQC is quantum by nature, it is expected to better capture quantum entanglement and learn the quantum phase structure of the target state more efficiently. Besides, sampling from the PQC is highly efficient as it can draw independent samples each time without a high rejection ratio in traditional Metropolis-Hasting sampling strategy. In summary, the VQNHE approach can be either referred to as the neural-network enhanced VQE or as the quantum-computing assisted VMC; it actually combines the advantages of both.

One of the promising future directions is to combine the VQNHE and quantum architecture search [43,65–70] or the adaptive VQE [71–76] in which the parametrized circuit *Ansatz* can be iteratively adjusted or grown to improve the overall performance for such a hybrid work flow. Moreover, it is worth theoretically investigating the noise resilience of the VQNHE, as relevant evidences emerge from hardware experiments in this work.

Conclusion.—In this Letter, we propose a VQNHE that combines nonunitary postprocessing with the PQC to improve upon VQE. The VQNHE uses a hybrid representation of quantum states in order to enhance the expressive power with limited quantum hardware resources, and it consistently outperforms the VQE in various tasks. We also outline a feasible protocol for implementing the VQNHE on real quantum hardware with rigorously proven efficiency. We demonstrate that the VQE with arbitrary nonunitary postprocessing can be accurately carried out with only polynomial overhead: an exponential improvement of efficiency that was deemed unlikely along the lines of prior proposals.

This work is supported in part by the NSFC under Grant No. 11825404 (S. X. Z., Z. Q. W., and H. Y.), the CAS Strategic Priority Research Program under Grant No. XDB28000000 (H. Y.), the MOSTC Grants No. 2018YFA0305604 and No. 2021YFA1400100 (H. Y.), Beijing Natural Science Foundation under Grant No. Z180010 (H. Y.), and Beijing Municipal Science and Technology Commission under Grant No. Z181100004218001 (H. Y.).

*These two authors contributed equally to this work.
†kimhsieh@tencent.com
‡yaohong@tsinghua.edu.cn

[1] R. P. Feynman, Simulating physics with computers, Int. J. Theor. Phys. **21**, 467 (1982).
[2] M. A. Nielsen and I. L. Chuang, *Quantum Computation and Quantum Information* (Cambridge University Press, Cambridge, England, 2010).
[3] J. D. Whitfield, J. Biamonte, and A. Aspuru-Guzik, Simulation of electronic structure Hamiltonians using quantum computers, Mol. Phys. **109**, 735 (2011).
[4] I. M. Georgescu, S. Ashhab, and F. Nori, Quantum simulation, Rev. Mod. Phys. **86**, 153 (2014).
[5] D. Wecker, B. Bauer, B. K. Clark, M. B. Hastings, and M. Troyer, Gate-count estimates for performing quantum chemistry on small quantum computers, Phys. Rev. A **90**, 022305 (2014).
[6] J. Preskill, Quantum computing in the NISQ era and beyond, Quantum **2**, 79 (2018).
[7] S. Endo, Z. Cai, S. C. Benjamin, and X. Yuan, Hybrid quantum-classical algorithms and quantum error mitigation, J. Phys. Soc. Jpn. **90**, 032001 (2021).
[8] M. Cerezo, A. Arrasmith, R. Babbush, S. C. Benjamin, S. Endo, K. Fujii, J. R. McClean, K. Mitarai, X. Yuan, L. Cincio, and P. J. Coles, Variational quantum algorithms, Nat. Rev. Phys. **3**, 625 (2021).
[9] K. Bharti, A. Cervera-Lierta, T. H. Kyaw, T. Haug, S. Alperin-Lea, A. Anand, M. Degroote, H. Heimonen, J. S. Kottmann, T. Menke, W.-K. Mok, S. Sim, L.-C. Kwek, and A. Aspuru-Guzik, Noisy intermediate-scale quantum (NISQ) algorithms, Rev. Mod. Phys. **94**, 015004 (2022).
[10] A. Peruzzo, J. McClean, P. Shadbolt, M.-H. Yung, X.-Q. Zhou, P. J. Love, A. Aspuru-Guzik, and J. L. O'Brien, A variational eigenvalue solver on a photonic quantum processor, Nat. Commun. **5**, 4213 (2014).
[11] P. J. J. O'Malley *et al.*, Scalable Quantum Simulation of Molecular Energies, Phys. Rev. X **6**, 031007 (2016).
[12] J. R. McClean, J. Romero, R. Babbush, and A. Aspuru-Guzik, The theory of variational hybrid quantum-classical algorithms, New J. Phys. **18**, 023023 (2016).
[13] C. Hempel, C. Maier, J. Romero, J. McClean, T. Monz, H. Shen, P. Jurcevic, B. P. Lanyon, P. Love, R. Babbush, A. Aspuru-Guzik, R. Blatt, and C. F. Roos, Quantum

Chemistry Calculations on a Trapped-Ion Quantum Simulator, Phys. Rev. X **8**, 031022 (2018).
[14] J.-G. Liu, Y.-H. Zhang, Y. Wan, and L. Wang, Variational quantum eigensolver with fewer qubits, Phys. Rev. Research **1**, 023025 (2019).
[15] Y. Cao, J. Romero, J. P. Olson, M. Degroote, P. D. Johnson, M. Kieferová, I. D. Kivlichan, T. Menke, B. Peropadre, N. P. D. Sawaya, S. Sim, L. Veis, and A. Aspuru-Guzik, Quantum chemistry in the age of quantum computing, Chem. Rev. **119**, 10856 (2019).
[16] S. McArdle, S. Endo, A. Aspuru-Guzik, S. C. Benjamin, and X. Yuan, Quantum computational chemistry, Rev. Mod. Phys. **92**, 015003 (2020).
[17] B. Bauer, S. Bravyi, M. Motta, and G. Kin-Lic Chan, Quantum algorithms for quantum chemistry and quantum materials science, Chem. Rev. **120**, 12685 (2020).
[18] O. Higgott, D. Wang, and S. Brierley, Variational quantum computation of excited states, Quantum **3**, 156 (2019).
[19] K. M. Nakanishi, K. Mitarai, and K. Fujii, Subspace-search variational quantum eigensolver for excited states, Phys. Rev. Research **1**, 033062 (2019).
[20] Y. Li and S. C. Benjamin, Efficient Variational Quantum Simulator Incorporating Active Error Minimization, Phys. Rev. X **7**, 021050 (2017).
[21] X. Yuan, S. Endo, Q. Zhao, Y. Li, and S. C. Benjamin, Theory of variational quantum simulation, Quantum **3**, 191 (2019).
[22] S. McArdle, T. Jones, S. Endo, Y. Li, S. C. Benjamin, and X. Yuan, Variational ansatz-based quantum simulation of imaginary time evolution, npj Quantum Inf. **5**, 75 (2019).
[23] C. Cîrstoiu, Z. Holmes, J. Iosue, L. Cincio, P. J. Coles, and A. Sornborger, Variational fast forwarding for quantum simulation beyond the coherence time, npj Quantum Inf. **6**, 82 (2020).
[24] S.-H. Lin, R. Dilip, A. G. Green, A. Smith, and F. Pollmann, Real- and imaginary-time evolution with compressed quantum circuits, PRX Quantum **2**, 010342 (2021).
[25] S. Endo, J. Sun, Y. Li, S. C. Benjamin, and X. Yuan, Variational Quantum Simulation of General Processes, Phys. Rev. Lett. **125**, 010501 (2020).
[26] M. Benedetti, M. Fiorentini, and M. Lubasch, Hardware-efficient variational quantum algorithms for time evolution, Phys. Rev. Research **3**, 033083 (2021).
[27] C.-K. Lee, P. Patil, S. Zhang, and C.-Y. Hsieh, A neural-network variational quantum algorithm for many-body dynamics, Phys. Rev. Research **3**, 023095 (2021).
[28] F. Arute *et al.*, Quantum supremacy using a programmable superconducting processor, Nature (London) **574**, 505 (2019).
[29] H.-S. Zhong *et al.*, Quantum computational advantage using photons, Science **370**, 1460 (2020).
[30] A. G. Taube and R. J. Bartlett, New perspectives on unitary coupled-cluster theory, Int. J. Quantum Chem. **106**, 3393 (2006).
[31] D. Wecker, M. B. Hastings, and M. Troyer, Progress towards practical quantum variational algorithms, Phys. Rev. A **92**, 042303 (2015).
[32] A. Kandala, A. Mezzacapo, K. Temme, M. Takita, M. Brink, J. M. Chow, and J. M. Gambetta, Hardware-efficient variational quantum eigensolver for small molecules and quantum magnets, Nature (London) **549**, 242 (2017).
[33] A. J. McCaskey, Z. P. Parks, J. Jakowski, S. V. Moore, T. D. Morris, T. S. Humble, and R. C. Pooser, Quantum chemistry as a benchmark for near-term quantum computers, npj Quantum Inf. **5**, 99 (2019).
[34] J.-G. Liu and L. Wang, Differentiable learning of quantum circuit Born machines, Phys. Rev. A **98**, 062324 (2018).
[35] J.-G. Liu, L. Mao, P. Zhang, and L. Wang, Solving quantum statistical mechanics with variational autoregressive networks and quantum circuits, Mach. Learn. **2**, 025011 (2021).
[36] G. Verdon, J. Marks, S. Nanda, S. Leichenauer, and J. Hidary, Quantum hamiltonian-based models and the variational quantum thermalizer algorithm, arXiv:1910.02071.
[37] C. Y. Hsieh, Q. Sun, S. Zhang, and C. K. Lee, Unitary-coupled restricted Boltzmann machine ansatz for quantum simulations, npj Quantum Inf. **7**, 19 (2021).
[38] M. Benedetti, B. Coyle, M. Fiorentini, M. Lubasch, and M. Rosenkranz, Variational Inference with a Quantum Computer, Phys. Rev. Applied **16**, 044057 (2021).
[39] J. Rivera-Dean, P. Huembeli, A. Acín, and J. Bowles, Avoiding local minima in variational quantum algorithms with neural networks, arXiv:2104.02955.
[40] G. Torlai, G. Mazzola, G. Carleo, and A. Mezzacapo, Precise measurement of quantum observables with neural-network estimators, Phys. Rev. Research **2**, 022060(R) (2020).
[41] E. R. Bennewitz, F. Hopfmueller, B. Kulchytskyy, J. Carrasquilla, and P. Ronagh, Neural error mitigation of near-term quantum simulations, arXiv:2105.08086.
[42] G. Li, Z. Song, and X. Wang, VSQL: Variational shadow quantum learning for classification, arXiv:2012.08288.
[43] S.-X. Zhang, C.-Y. Hsieh, S. Zhang, and H. Yao, Neural predictor based quantum architecture search, Mach. Learn. **2**, 045027 (2021).
[44] G. Mazzola, P. J. Ollitrault, P. K. Barkoutsos, and I. Tavernelli, Nonunitary Operations for Ground-State Calculations in Near-Term Quantum Computers, Phys. Rev. Lett. **123**, 130501 (2019).
[45] R. Jastrow, Many-body problem with strong forces, Phys. Rev. **98**, 1479 (1955).
[46] A. Zen, E. Coccia, Y. Luo, S. Sorella, and L. Guidoni, Static and dynamical correlation in diradical molecules by quantum Monte Carlo using the Jastrow antisymmetrized geminal power ansatz, J. Chem. Theory Comput. **10**, 1048 (2014).
[47] C. Genovese, A. Meninno, and S. Sorella, Assessing the accuracy of the Jastrow antisymmetrized geminal power in the H^4 model system, J. Chem. Phys. **150**, 084102 (2019).
[48] F. Benfenati, G. Mazzola, C. Capecci, P. K. Barkoutsos, P. J. Ollitrault, I. Tavernelli, and L. Guidoni, Improved accuracy on noisy devices by non-unitary variational quantum eigensolver for chemistry applications, arXiv:2101.09316.
[49] See Supplemental Material at http://link.aps.org/supplemental/10.1103/PhysRevLett.128.120502 for measurement efficiency proof for VQNHE, comparison with previous methods in terms of complexity scaling, VQNHE formalism with complex neural function, and technical details of quantum simulation on spin and molecule systems with numerical methods and hardware experiments.

[50] J. Li, X. Yang, X. Peng, and C.-P. Sun, Hybrid Quantum-Classical Approach to Quantum Optimal Control, Phys. Rev. Lett. **118**, 150503 (2017).
[51] K. Mitarai, M. Negoro, M. Kitagawa, and K. Fujii, Quantum circuit learning, Phys. Rev. A **98**, 032309 (2018).
[52] M. Schuld, V. Bergholm, C. Gogolin, J. Izaac, and N. Killoran, Evaluating analytic gradients on quantum hardware, Phys. Rev. A **99**, 032331 (2019).
[53] The open source implementation of VQNHE can be found at https://github.com/refraction-ray/tensorcircuit, we also utilize Psi4 [54] and OpenFermion [55] in the calculation of molecules.
[54] J. M. Turney, A. C. Simmonett, R. M. Parrish, E. G. Hohenstein, F. A. Evangelista, J. T. Fermann, B. J. Mintz, L. A. Burns, J. J. Wilke, M. L. Abrams, N. J. Russ, M. L. Leininger, C. L. Janssen, E. T. Seidl, W. D. Allen, H. F. Schaefer, R. A. King, E. F. Valeev, C. D. Sherrill, and T. D. Crawford, Psi4: An open-source *ab initio* electronic structure program, Wiley Interdiscip. Rev. **2**, 556 (2012).
[55] J. R. McClean *et al.*, OpenFermion: The electronic structure package for quantum computers, 3arXiv:1710.07629.
[56] K. Choo, A. Mezzacapo, and G. Carleo, Fermionic neural-network states for ab-initio electronic structure, Nat. Commun. **11**, 2368 (2020).
[57] M. Steudtner and S. Wehner, Fermion-to-qubit mappings with varying resource requirements for quantum simulation, New J. Phys. **20**, 063010 (2018).
[58] W. L. McMillan, Ground state of liquid He^4, Phys. Rev. **138**, A442 (1965).
[59] D. Ceperley, G. V. Chester, and M. H. Kalos, Monte Carlo simulation of a many-fermion study, Phys. Rev. B **16**, 3081 (1977).
[60] G. Carleo and M. Troyer, Solving the quantum many-body problem with artificial neural networks, Science **355**, 602 (2017).
[61] T. Westerhout, N. Astrakhantsev, K. S. Tikhonov, M. I. Katsnelson, and A. A. Bagrov, Generalization properties of neural network approximations to frustrated magnet ground states, Nat. Commun. **11**, 1593 (2020).
[62] M. Bukov, M. Schmitt, and M. Dupont, Learning the ground state of a non-stoquastic quantum Hamiltonian in a rugged neural network landscape, SciPost Phys. **10**, 147 (2021).
[63] C.-Y. Park and M. J. Kastoryano, Are neural quantum states good at solving non-stoquastic spin Hamiltonians?, arXiv:2012.08889.
[64] X. Liang, S.-J. Dong, and L. He, Hybrid convolutional neural network and projected entangled pair states wave functions for quantum many-particle states, Phys. Rev. B **103**, 035138 (2021).
[65] S.-X. Zhang, C.-Y. Hsieh, S. Zhang, and H. Yao, Differentiable quantum architecture search, arXiv:2010.08561.
[66] L. Li, M. Fan, M. Coram, P. Riley, and S. Leichenauer, Quantum optimization with a novel Gibbs objective function and ansatz architecture search, Phys. Rev. Research **2**, 023074 (2020).
[67] Y. Du, T. Huang, S. You, M.-H. Hsieh, and D. Tao, Quantum circuit architecture search: Error mitigation and trainability enhancement for variational quantum solvers, arXiv:2010.10217.
[68] Z. Lu, P.-X. Shen, and D.-L. Deng, Markovian Quantum Neuroevolution for Machine Learning, Phys. Rev. Applied **16**, 044039 (2021).
[69] M. Bilkis, M. Cerezo, G. Verdon, P. J. Coles, and L. Cincio, A semi-agnostic ansatz with variable structure for quantum machine learning, arXiv:2103.06712.
[70] E.-J. Kuo, Y.-L. L. Fang, and S. Y.-C. Chen, Quantum architecture search via deep reinforcement learning, arXiv:2104.07715.
[71] H. R. Grimsley, S. E. Economou, E. Barnes, and N. J. Mayhall, An adaptive variational algorithm for exact molecular simulations on a quantum computer, Nat. Commun. **10**, 3007 (2019).
[72] A. G. Rattew, S. Hu, M. Pistoia, R. Chen, and S. Wood, A domain-agnostic, noise-resistant, hardware-efficient evolutionary variational quantum eigensolver, arXiv:1910.09694.
[73] D. Chivilikhin, A. Samarin, V. Ulyantsev, I. Iorsh, A. R. Oganov, and O. Kyriienko, MoG-VQE: Multiobjective genetic variational quantum eigensolver, arXiv:2007.04424.
[74] Y. S. Yordanov, V. Armaos, C. H. Barnes, and D. R. Arvidsson-Shukur, Iterative qubit-excitation based variational quantum eigensolver, Commun. Phys. **4**, 228 (2021).
[75] S. Sim, J. Romero, J. F. Gonthier, and A. A. Kunitsa, Adaptive pruning-based optimization of parameterized quantum circuits, Quantum Sci. Technol. **6**, 025019 (2021).
[76] D. Claudino, J. Wright, A. J. McCaskey, and T. S. Humble, Benchmarking adaptive variational quantum eigensolvers, Frontiers of chemistry **8**, 1 (2020).